Tutors

Dr. Joan Formosa Mitjans
Departament de Ciència i Enginyeria de Materials

Sr. Alex Maldonado Alameda

Departament de Ciència i Enginyeria de Materials

UNIVERSITAT DE BARCELONA

Grau d'Enginyeria de Materials

Treball Final de Grau

Development of magnesium phosphate cement mortars formulated with reactive silica

Desarrollo de morteros de cemento de fosfato de magnesio formulados con sílice reactiva

Eduard Cosialls Borràs

June 2018

UNIVERSITAT DE BARCELONA

Dos campus d'excel·lència internacional

B:KC Barcelona Knowledge Campus

HUBC Health Universitat de Barcelona Campus

REPORT

CONTENTS

1. GLOSSARY

MPC	Magnesium Phosphate Cement
Lg-MgO	Low grade Magnesium Oxide
PC8	Lg-MgO used in the project
MKP	Monopotassium Phosphate
CSP	Ceramics, Stone and Porcelain
XRF	X-ray Fluorescence
XRD	X-ray Diffraction
FTIR-ATR	Fourier Transformed Infrared Spectroscopy
DoE	Design of Experiments
OPC	Ordinary Portland cement
CBPC	Chemically Bonded Phosphate Ceramics
MOE	Modulus of Elasticity
FS	Flexural Strength
CS	Compressive Strength
SEM	Scanning Electron Microscope
EPS	Expanded Polystyrene
W/C	Water to Cement
EDS	Energy-dispersive X-ray Spectroscopy

2. SUMMARY

The construction sector has been in upwgrowing these last years and consequently the contamination is at a level that takes society to concern. That is why nowadays it is a challenge for engineers and scientists to develop sustainable and eco-friendly construction materials.

This research project aims to replace portland cement (OPC) using Chemically Bonded Phosphate Ceramics (CBPC). This cement is characterized by having a spontaneous and highly exothermic reaction that leads to a very fast setting. It also uses by-products such as magnesium oxide (Lg-MgO) and Ceramic, Stone and Porcelain (CSP) to make the material more sustainable and at the same time have a more competitive price in the market. It is wanted to analyze if the CSP reacts with the structure of the MPC known as k-struvite.

To reach the optimal formulation, different influence factors are determined in the mortar and they are assigned important values through an Experiment Design (DoE). The results show that an increase of CSP increases mechanical and physical properties, but reactivity with k-struvite is unclear. The resulting MPC can be used as a repairing mortar.

3. RESUMEN

El sector de la construcción ha estado creciendo en los últimos años y como consecuencia la contaminación está en un nivel preocupante para nuestra sociedad. Es por eso que hoy en día es un desafío para los ingenieros y científicos el desarrollo de materiales de construcción sostenibles y ecológicos.

Este proyecto de investigación tiene como objetivo reemplazar el cemento portland (OPC) utilizando cerámica de fosfato químicamente unida (CBPC). Este cemento se caracteriza por tener una reacción espontánea y altamente exotérmica que conduce a un tiempo de puesta en servicio y fraguado muy corto.

También se utilizan subproductos como el óxido de magnesio (Lg-MgO) y cerámica, piedra y porcelana (CSP) para hacer que el material sea más sostenible y, al mismo tiempo, tenga un precio más competitivo en el mercado. Se quiere analizar si el CSP reacciona con la estructura del MPC conocida como k-estruvita. Para alcanzar la formulación óptima, se determinan diferentes factores de influencia en el mortero y se les asignan valores importantes a través de un diseño de experimentos (DoE).

Los resultados muestran que un aumento de CSP aumenta las propiedades mecánicas y físicas, pero la reactividad con k-estruvita no está clara. El MPC resultante se puede usar como un mortero de reparación.

4. INTRODUCTION

The population has been in upgrowing for the last century, and as a direct result the construction sector is in the rise. This sector has been the origin of the global contamination, by producing a high amount of waste and polluting the environment in doing so. The cement factories are, behind the steel industry, the most polluting industry generating the 12% of the total CO_2 emissions of the planet.

In 2015, the consumption of waste in the EU-28 represented that 41% of the energy consumption came from the cement sector[1]. 2.7Mt of waste were generated from this sector and only a small part was brought into recycling plants.

Nowadays it is a challenge to engineers and scientists to develop sustainable and eco-friendly materials. Green concrete could be an eco-efficient alternative to concrete made using ordinary Portland cement (OPC), reducing CO_2 emissions substantially.

The aim of this project is to develop and characterize a sustainable alternative to most contaminant cements. In order to do so, by-products will be used to reach the ecological and environmental benefit we want to achieve. By doing so, the price will be reduced, even though the OPC keeps being cheaper due to its global use in industries.

The chosen cement to accomplish the goal is the phosphate cement, using a magnesium by-product obtained in the calcination process of magnesia (MgO) and the scrap of the glass recycling industry.

The goal to create a new crystalline structure for the magnesium phosphate cement by adding a source of aluminosilicates in order to improve the mechanical properties.

4.1. CHEMICAL PHOSPHATE CEMENTS

Chemical phosphate cements, also known as Chemically Bonded Phosphate Ceramics (CBPC), are of main interest for its unique properties, such as rapid setting,

good volume stability, advantageous bonding strength, high early strength and extensive temperature stability[2,3,4].

They distinguish themselves from hydraulic cements, such as OPC, in the way they harden. Hydraulic cements need to react with water in order to hydratate and harden while CBPC belong to the acid-base cements group. It is not as expensive as many acid-base cements because the raw materials are well scattered in the Earth's crust. OPC has an alkaline pH while the CBPC are stable in a wide pH range.

The acid-base reaction that harden such cements (Eq. 1) is obtained between a metal cation and a source of phosphate acid in an aqueous medium [5,6].

$$MO_x + nH_3PO_4 + nHmH2O \rightarrow MH_{3n-2x}(PO_4) + (m + n)\,H_2O \quad (1)$$

Where m is an arbitrary value that determines the amount of water added to the reaction, x corresponds to the valence of the metal M and $n \geq 1/3x$.

Wagh[7] was the first to describe how phosphate cements harden. He explains that the kinetics is very similar to the manufacturing process of ceramics by the sol-gel method. The following figure shows the formation mechanism CBPC[5]

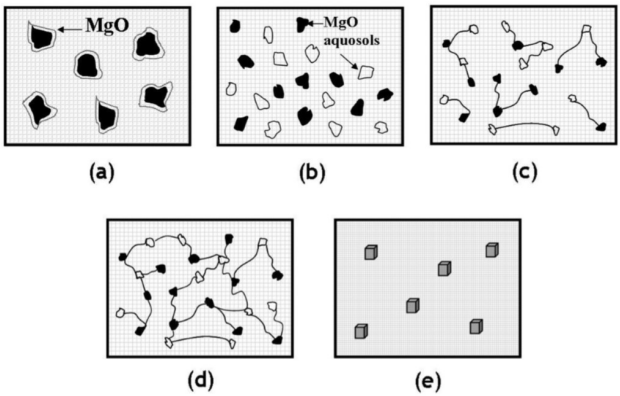

Figure 1. (a) Dissolution of oxides (b) Formation of aquosols (c) Acid-base reaction and condensation (d) percolation and formation of gel (e) Crystallization and saturation of gel into a ceramic.

-First, the metallic oxides are agitated and dissolved slowly in an acid solution. This causes the release of metal cations and anions containing oxygen (Fig. 1a).

-Then cations form aquosols by hydrolysis when reacting with water (Fig. 1b).

-Next, the formed aquosols react with aqueous phosphate anions to form hydro phosphate salts (Fig. 1c) .

-As the reaction proceeds, the salts form a network of molecules in the aqueous solution that leads to the formation of a gel (Fig. 1d).

-Finally more gel is formed until it crystallizes around the metallic oxide grains generating a well-connected crystal lattice, typical of a ceramic (Fig. 1e).

One of the first applications of CBPC was as dental cement due to its biocompatibility with the human body, although it is no longer used. It was employed in temporary fillings or to cement prostheses but the manipulation was very sensitive to mixing, therefore the liquid-powder ratio affected substantially its mechanical properties and its solubility. It also produces an exothermic reaction, which damages the pulpal vitality and the mucous membranes surrounding the tooth.[8]

4.1.1.Magnesium Phosphate Cements

The material used in this project for the formation of the magnesium phosphate cement (MPC) is magnesium oxide (MgO). It comes from dolomite (magnesium carbonate and calcium carbonate) and magnesite (magnesium carbonate). It is the most commonly used in phosphate cements due to its abundance in the earth's crust and low solubility (a value between CaO and SiO_2 or FeO)[7].

It is a key factor, since the material must have a sufficiently high solubility to make the formation of the gel but low to be able to crystallize and exothermic reaction that requires a slow heat production to allow the phosphate gel to precipitate [9].The source of anions (phosphate) that will be used is the monopotassium phosphate (MKP).

$$MgO + KH_2PO_4 + 5H_2O \rightarrow KMg(PO)_4 \cdot 6H_2O \quad (2)$$

The resulting structure is k-struvite ($KMgPO_4 \cdot 6H_2O$). This structure is a salt of magnesium phosphate and potassium and is equivalent to the orthorhombic pyramidal structure of the struvite ($NH_4MgPO_4 \cdot 6H_2O$) but the potassium ions (K^+) replace the ammonium ions (NH_4^+), as the ionic radium is almost identical[10].

MPC also has a non-crystalline phase, not all MgO reacts, so that particles remain converting the cement into a mortar. The product obtains better mechanical properties since it is mortar because the fine aggregate acts as a filler [6,11]. It behaves as a ceramic due to its crystalline structure and does not suffer dehydratation until 180°C[9].

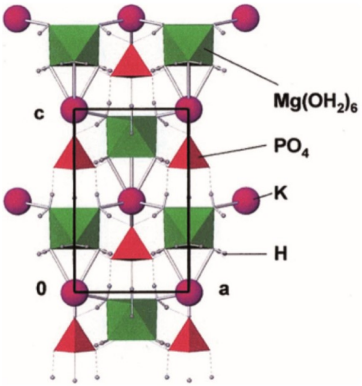

Figure 2. K-Struvite crystalline structure[10]

It is 3 times more expensive than the OPC but 4 times less polluting an it can be set under water.

Currently the phosphate cement, or phosphate mortar, is used as mortar for joints or as a repair mortar in roads, pavements and airports. Due to its short setting time and mechanical properties, its start-up can be very quick[2]. It has also been found as fire protective coatings and in the nuclear industry as stabilizer of radioactive and toxic waste[5].

4.2. CERAMIC STONE AND PORCELAIN (CSP)

The Ceramic, Stone and Porcelain known as CSP is the fraction that cannot be recycled from the glass because its size is small or because it has paper stuck or impurities. It has a high content of glass, metals, organics and CSP (ceramics, stone and porcelain). Especially in the case of CSP, it is a problem for glass recycling companies because they have a melting point greater than the glass and therefore do not melt, making it difficult to recover. In the early 1970s until mid 1980s, manual sorting ("handpicking") was the only method to reduce CSP[12]. Today automated optical sorting is used to classify clean cullets from contaminated cullets (fig. 3).

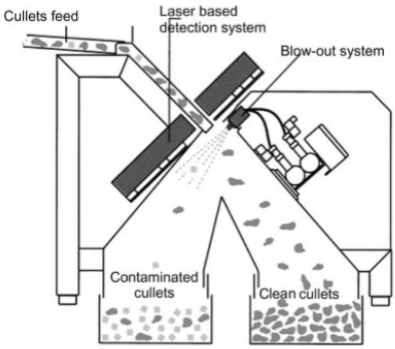

Figure 3. Chromatic separator[13]

The bottle but and bottlenecks are more dense and therefore have a darker tone. Chromatic separators do not detect them.[14,13] That is the reason why contaminant glass cullet is over 80% glass. Therefore, we can say that CSP are mostly aluminosilicates.

Recycling companies do not accept recycled glass if it contains more than 20 grams per tonne of CSP. They are currently treated as non-profitable material that goes to landfill. By giving it an application we are making the mortar cheaper and more sustainable.

4.3. DESIGN OF EXPERIMENTS (DOE)

The mortar will be developed with the help of Design of Experiments (DoE). It is a tool that is used to determine which experiments will allow us to test out our hypothesis and which will not. With the minimum number of experiments, it can obtain a lot of information and predict the best formulation based on the parameters. It can identify the possible interactions between two factors and It will also be used to distinguish between factors that will affect the experiment and those that will not while saving time in the process[15,16].

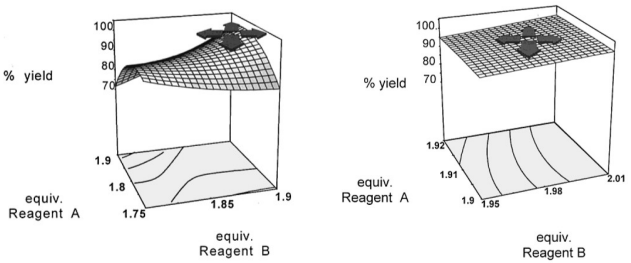

Figure 4. Possible response surface designs[16]

4.4. OBJECTIVES

The aim of the work is to react the amorphous silica and aluminosilicates of the glass cullet with the structure that forms the phosphate cements with the magnesium by-product to improve the mechanical properties.

The suitable formulation obtained with the design of experiments will be characterized to determine if the aluminosilicates react with the k-struvite or only act as filler and then we will be able to interpret the applications.

- Use the design of experiments in order to do the least number of formulations in order to obtain the material with the best properties. The project parameters will be the water-cement proportion and the percentage of glass cullet.

- Evaluate the mechanical properties of the cement in relation to its percentage of class cullet (compression strength, flexural strength, MoE, volumetric contraction).

- Characterize the phosphate cement to determine if a new structure is formed or if the silica acts as filler.

- Find a practical application for the resulting material.

5. EXPERIMENTAL PROCEDURE

The raw materials for the formulation of MPC and the incorporation of CSP are shown in this section. It also describes the methodology used to carry out the tests as well as the preparation of the samples and formulations. All the raw materials characterizations are presented because they are needed in order to prepare the MPC. MPC characterizations are shown in the section 6. The equipment that is used to characterize the products and determine the properties are also presented.

5.1. CHARACTERIZATION OF MATERIALS

5.1.1. Monopotassium phosphate (MKP)

Monopotassium phosphate (KH_2PO_4), also known as potassium dihydrogen phosphate, is a salt commonly used in pesticides, food additives, and fertilizers. It is used in the formation of the MPC as the source of phosphate anions. The supplier of this crystalline white powder is Rotem Amfert Negev Ltd and the brand's name is MKP. The use of the MKP reduces the final cost of the MPC, as it is not considered as a reactive grade chemical but as a food grade product. It is soluble in water, has a basic pH and a density of 2.34 g/cm³.

5.1.2. By-product of magnesium oxide (LG-MgO)

The metallic ion that will be used is a by-product of magnesium oxide (MgO) known as low grade magnesium oxide (LG-MgO). By using a by-product as raw material the final cost of the MPC is reduced and environmental benefits are also obtained, as the extraction of pure MgO diminishes.

It is provided by Magnesitas Navarra S.A., a company that obtains magnesium oxide from the calcination of natural ores rich in magnesite (MgCO3). The calcination is carried out at temperatures above 1100°C which generates fly ash that is retained in the

bag filter. This brown coloured cyclone powder is the Lg-MgO, known by the company as PC8, and corresponds to the 30% of the production of MgO. The calcination process used in Magnesitas Navarra S.A. is shown in figure 5. Although is not a pure product, it is reactive enough to obtain MPC as prove Formosa et al[17].

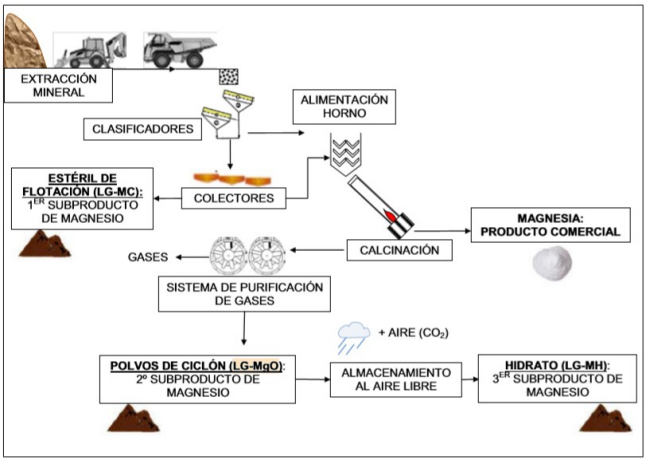

Figure 5. Calcination process of natural magnesite[18]

5.1.2.1 X-ray fluorescence (XRF)

The PC8's composition is determined using a x-ray fluorescence spectrometer (XRF) with the equipment Philips PW2400, a wavelength dispersion X-ray sequential spectrophotometer (WDXRF). The results show the most stable oxide (Table 1).

Table 1. PC8 composition

Composition	MgO	CaO	SO_3	Fe_2O_3	SiO_2	Al_2O_3	LOI
%	61,7	9,32	6,55	2,43	2,7	0,55	16,73

The decrease in weight of MgO causes a change of stoichiometry in the reaction of formation of MPC (Eq. 2) It will no longer be a 50 to 50 ratio but rather the source of cations must be increased and the MKP content decreased. This favours the resulting price of the MPC since the PC8 is about nine times cheaper than the MKP.

The loss on ignition (LOI) is attributable to potential carbonates and hydrated phases present in the PC8.

5.1.2.2 Particle size distribution

It is important to take into account the particle size of the cation source due to its effect on the speed of the reaction of formation of the phosphate cement. In figure 6 the volumetric distribution is compared to the particle size. An unimodal curve with a maximum of 30 microns is observed. It is also observed that the maximum size of the particles is less than 200 microns.

It is obtained a dispersion laser Beckman Coulter LS 13.320 equipment. The sample is dispersed in an ultrasound bath for five minutes, using acetone as a bearing medium.

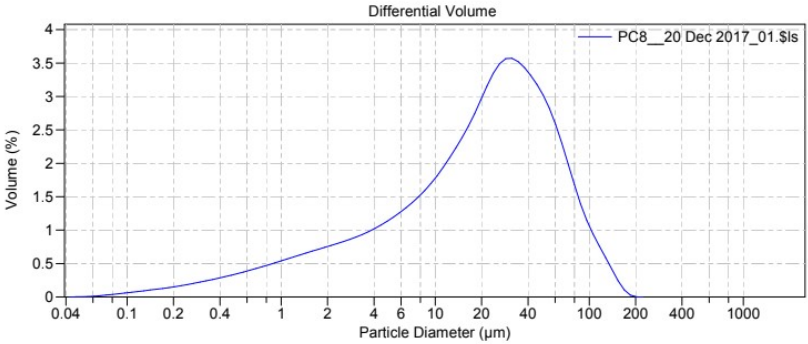

Figure 6. Distribution of percentages in volume of particle size of LG-MgO

In the following table is shown the diameter below which the corresponding percentage of the particles measured in volume is found.

Table 2. Percentages in volume of particle size of LG-MgO

%	<10	<25	<50	<75	<95
µm	1.68	6.99	21.09	41.55	87.57

The smaller the size of the particles more reactive is the MgO. This results show that it is a by-product with a small particle size, attributable to the process of obtaining the PC8.

5.1.2.3 X-Ray diffraction (XRD)

X-ray diffraction (DRX) is performed to analyze the present elements of PC8 qualitatively (fig. 7).

The presence of periklase as a major source is observed, such as quartz (SiO_2), dolomite [$CaMg(CO_3)_2$], magnesite [$Mg(CO_3)$] not calcined, and calcite [$Ca(CO_3)$] coming from natural magnesite. The anhydrite [$CaSO_4$)] is generated during the calcination of dolomite.

The test is performed using a Siemens D-500 diffractometer with BraggBrentano geometry from a sample of the PC8.

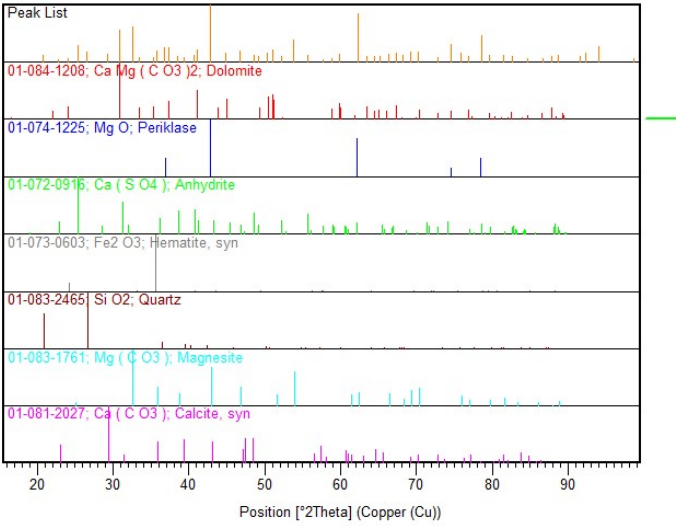

Figure 7. Crystalline phases determined by XRD

5.1.2.4. BET Surface Area

The analysis of the surface (BET) provides information about the active surface of the sample that is studied and as a result, the reactivity that presents. It is proven that a greater specific surface BET contributes to greater reactivity and therefore a faster hardening[4].

The specific area of the PC8 sample is 7.329 m^2/g. Compared to other commercial magnesia, which present values around 100 m^2/g it seems clear that this Lg-MgO has a very low reactivity. This low value can be justified due to the calcination to which this product was subjected during its obtaining. These results are obtained using a Micromeritics Tristar 3000 equipment.

5.1.3. Ceramic, Stone and Porcelain (CSP)

The supplier of the Ceramic, Stone and Porcelain (CSP) is the company Daniel Rosas S.A..This glass waste is cost free since the current CSP goes to landfill and the company saves this step by letting us experiment with the material. The materials that are present in CSP are shown in figure 8 below:

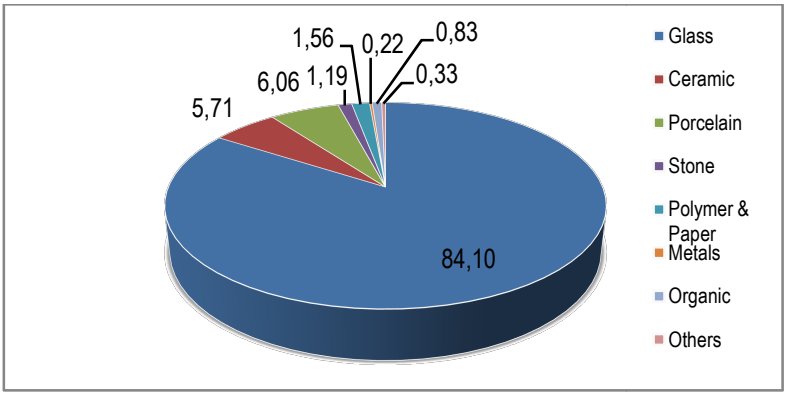

Figure 8. Percentages of the materials present in CSP

5.1.3.1 X-ray fluorescence (XRF)

The CSP composition is determined by using a x-ray fluorescence spectrometer (XRF) with the equipment Philips PW2400, a wavelength dispersion X-ray sequential spectrophotometer (WDXRF). The results show the most stable oxide (Table 3).

Table 3. Main components in CSP powder

Composition	SiO_2	CaO	Na_2O	Al_2O_3	MgO	K_2O	Fe_2O_3	TiO_2	P_2O_5	MnO	LOI
%	70,78	9,37	11,15	4,81	1,61	0,94	0,57	0,13	0,04	0,02	0,99

As it is expected, SiO_2 is the main component in CSP, while elements like CaO, Na_2O or K_2O are exist because they are present in bottle glass. Al_2O_3 should be the second major component in order to promote reactivity with MPC. The loss on ignition (LOI) is attributable to the thermal organic components.

5.1.3.2 Particle size distribution

Once we obtain CSP in powder form as it is shown in section 5.2.1 a particle size distribution is made. It is obtained a dispersion laser Beckman Coulter LS 13.320 equipment from a sample of CSP.

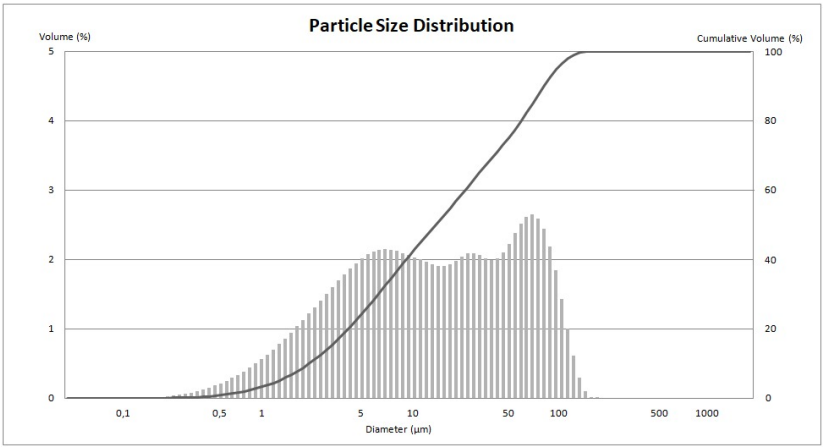

Figure 9. Particle size distribution of CSP

By having a powder with low a diameter size we favour the reactivity with the MPC. If the CSP does not react with k-struvite, different particle sizes are desired in order to obtain a balanced Fuller curve.

5.1.4.MPC

5.1.4.1. X-ray diffraction (XRD)

An X-ray diffraction (XRD) of a phosphate cement without CSP is performed and compared with the optimum formulation obtained. It is carried out with a diffractometer from Siemens D-500 with BraggBrentano geometry. The objective is to see if a structure other than k-struvite is formed.

5.1.4.2. Infrared Spectroscopy (FTIR-ATR)

A characterization of the composition and structure of MPC formulations (without CSP and optimal) is performed through a FTIR-ATR Spectrum equipment (Fourier Transform Infrared Spectroscopy and Attenuated Total Reflectance).

The analysis with the FTIR-ATR device requires a simple preparation of the sample that consists of milling a small amount of each one of the pots with the help of an agate mortar. In order to increase the efficiency of the test, it is required to obtain a powder with a similar grain size, as well as place the same amount of powder on the measuring device (Fig.10). Once the test is finished the surface of the device is cleaned with ethanol.

Figure 10. Equipment used for the FTIR-ATR

This technique is a type of absorption spectrometry that uses the region of the average infrared electromagnetic spectrum for the identification of components or the composition of the samples, based on the specific vibration frequencies that present the chemical bonds of the material and that correspond to the energy levels of the molecule.

5.1.4.3. Scanning electron microscope (SEM)

A study of the morphology of MPC is realized. The formulations without CSP and the optimal formulation are observed in the scanning electron microscope (SEM) FEI Quanta 200. The main objective of the observation is to identify the phases present in the MPC, as well as analyze in a visual way how the CSP is positioned in the structure and if the inert phases of the PC8 have remained embedded in the phosphate and magnesium matrix.

Previously the samples had to be conditioned so that they were flat. To obtain the flatness and reduced size of the samples, a diamond disk cutter 150 Low Speed Diamond Saw of MTI (Fig. 11) is used, running at a speed of about 324 rpm, and cooling the disc with acetone. Due to the non-conductive nature of the studied material, it was necessary to cover the samples in graphite.

Figure 11. Low speed diamond saw

5.1.5 Formulations

Design of experiments (DoE) is used to know the influence of different factors in the mechanical properties. These factors are the ratio between MKP and PC8, the amount in percentage of CSP and the ratio between water and cement (W/C). To keep the experiment with only two variables the ratio between MKP and PC8 is fixed at 40/60, as it is shown to be the best ratio in J.Formosa studies[18].

To determine the range of CSP and water/cement ratio a small-scale experiment was carried out using cylindrical test tubes as shown in figure 12. The objective of the present study is to introduce the maximum amount of CSP without having to increase the cement water ratio too much, since a higher water content decreases the mechanical properties of the mortar. CSP will be considered as a filler, even though it might react with k-struvite. A parameter that also has to be controlled is the setting time, since increasing the arid content favours a faster setting. Taking into account that phosphate cement without CSP begins to set around two minutes, the ideal is that the formulation obtained does not deviate much from that number. Due to the small amount of CSP the maximum percentage introduced is 15%.

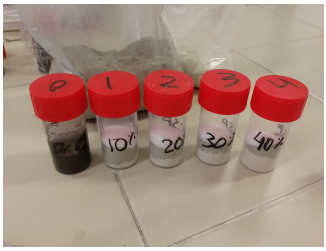

Figure 12. Test tubes with different CSP content

Once the preliminary tests are concluded, the matrix is obtained (Table 4). This matrix generates the minimum formulations to determine the optimal formulation taking into account the factors introduced.

By introducing the number of experiments that we want to do along with the matrix, the program will give the corresponding formulations with the different weight of CSP

and water. The properties that are analyzed by the program are contraction, density, flexural strength, and compression strength and Young modulus.

Table 4. Formulations generation matrix

	-1	0	1
W/C	0,34	0,36	0,38
% CSP	0	7,5	15
MKP/PC8		40/60	

5.2. PREPARATION OF RAW MATERIALS AND SAMPLES

In this section it is described the procedures to prepare MPC, from diminishing CSP's particle size to the mixing of the mortar.

5.2.1 CSP

To ensure that the CSP has a representative composition it is needed to quarter, divide in four parts the initial material (Fig.13a). A quarter is picked, consisting of 6 kg of CSP.

It is necessary to obtain the glass powder as small as possible to promote its reactivity. That's why the quartered material has been shredded to reduce the particle size up to a maximum of 2mm. Later, the ball mill is used with balls of alumina as it is shown in figure 14a. When it is milled with this type of mill, it is important that the media is of the same material as the sample to avoid contamination. As we have seen in section 5.1.3.1, the CSP has a percentage of Al_2O_3, so contamination is not a problem.

Figure 13. a) CSP before triturating and milling b) CSP powder

The ball mill is filled with 2 kg during 1 hour, then it is substituted with two more unmilled kilograms while the first round is sieved. CSP is classified by sizes, starting on 2mm and halving until 80µm is reached. Once the 6 initial kilograms are milled we continue to mill starting with the largest size (2mm) and once is all sieved we continue with the 1 mm size and so on. It is essential to mill all six kilograms of CSP because there are some materials like stone or porcelain that are easier to mill than ceramic and glass.

It is milled following this procedure during 39 hours to finally obtain two particle sizes; <80µm and <125 µm. It is reached a time were the CSP of this size cannot be diminished because it agglomerates. To reduce the size of <125 µm particles it is needed a more effective mill.

To mill the remaining powder the ring mill from the geology faculty is used. It works in all three axes and is capable to mill a maximum of 50 grams per round. After 52 rounds all the CSP has a particle size than less of 80 µm.

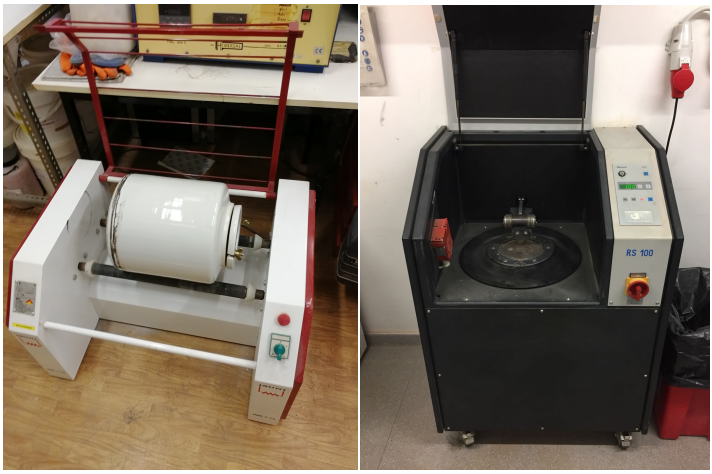

Figure 14. a) Ball mill b) Ring mill

5.2.2. Obtaining MPC

To prepare all the phosphate mortar formulations it is necessary to carry out a systematic procedure so that all the samples are prepared with the same conditions. Each step has to be timed, always carried out in the same order and the laboratory conditions of temperature and humidity have to be controlled to avoid possible variations in the final properties of the material. To prepare the MPC we use safety glasses and the mask, since we are working with glass powder with a size less than 80 microns that could be harmful.

First, the reactives (MKP, PC8 and CSP) are weighed in the pot in this order and mixed with a paddle for 30 seconds. The total solid weight is 2kg. Once mixed, the powder is completely brown and there is no trace of white or yellow powder. Then the corresponding water is weight and the pot is placed in the planetary mixer with the paddle placed as shown in figure 15a. The CSP is treated as non reactive, so instead of determining a water to solid ratio it is determined a water to cement ratio.

We put the water in the pot and close the planetary mixer. After 10 seconds it is turned on at low revolution for 30 seconds and then at high revolution for 30 more seconds. After this minute the team is stopped and for 20 seconds it is checked with a

palette that there is no dust at the bottom of the pot. Then the planetary mixer is turned on again on the high revolution mode for 60 seconds. As the base acid reaction proceeds, a characteristic smell of sulphates from PC8 is noticed. Once the 60 seconds are over the planetary mixer is stopped and we pour the MPC into expanded polystyrene (EPS) molds, from which we obtain three samples of 4x4x16cm. Then we use the shaking table (Fig.15b) during 10 seconds to finally top up with a palette to get the same height for the three samples. The shaking table serves to ensure homogenous weight in the three samples of mortar and to evacuate all the air during the mixing process. The samples are unmolded at 24 hours.

Figure 15. a) Planetary mixer b) Shaking table

5.3. DETERMINING OF PROPERTIES

5.3.1 Physical Characterization

It is important for mortars to know the retraction since it is necessary to know the useful dimensions. We want to determine this volumetric contraction, how the introduction of CSP affects the curing of cement and how affects having more water content to evaporate it. That is why the apparent density is determined in the fresh state and the samples are weighted at 24 hours and 7 days. In addition, the base and length of the samples are measured at 24 hours and at 7 days.

5.3.2 Modulus of Elasticity (MOE)

The determination of Young Modulus (MOE) is carried out by a non-destructive test by ultrasound, high frequency acoustic waves. The test works as follows: the delay times in the propagation of ultrasonic pulses are measured by traversing the distance between a transmitter and a receiver transducer through a sample of finite length, both coupled at the ends of the sample. Once the time spent and the length travelled have been known, the velocity of propagation of the ultrasonic pulses in longitudinal mode can be accurately found. The denser the material, the faster the wave propagation, so the material will be more rigid, with a greater Young's modulus. The samples are tested after 7 days. This testing follows the equation 3, were ρ is density an V is the longitudinal step velocity. V depends on the length of the sample and the resonance frequency, as observed in equation 4.

$$\mathrm{MOE} = \rho \cdot \mathrm{V}^2 \quad (3)$$

$$\mathrm{V} = 2 \cdot \mathrm{L} \cdot \mathrm{f} \quad (4)$$

The test carried out follows the UNE-EN 12504-4 standard and has been carried out with equipment provided by Saint Gobain Weber S.A. (Fig.16).

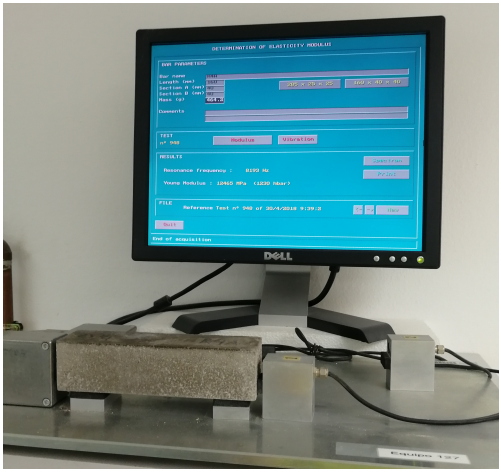

Figure 16. Modulus of elasticity determined by ultrasounds

5.3.3 Flexural Strength (FS)

To know the resistance to flexing of the mortar, a three-point flexion test will be performed after 7 days. A load of 20kN has been applied at a speed of 5 kg· s-1 until the rupture of the samples in two halves. The calculation of resistance to flexion at 3 points is performed following the equation 5.

$$FS = 1{,}5 \cdot \frac{\mathrm{F \cdot L}}{\mathrm{b \cdot d^2}} \quad (5)$$

Where F is the maximum applied load, L the distance between the 2 axes of support, b the width of the sample and d the height.

This testing follows the UNE-EN 1015-11 and is realized with the flexo-traction device Incotecnic MULTI-R1 belonging to the DIOPMA group. This type of machine has a mobile head that can be replaced with different ones, depending if we are doing flexural or compression testing.

The sample is positioned with the marked face perpendicular to the axis of flexion. This is because the marked face is the one that is not covered by the mold and the results may not be representative.

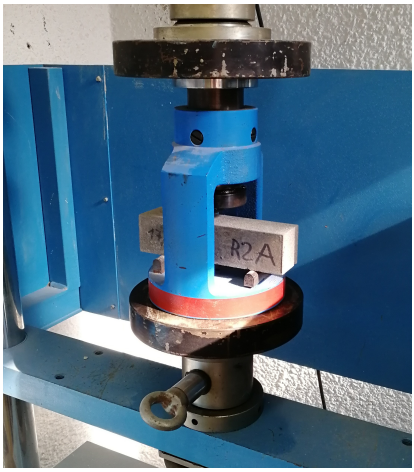

Figure 17. Flexo-traction testing device

5.3.4 Compressive Strength (CS)

To carry out the testing of the compression the same machine is used to test flexing, but the head is switched to a compression head(Fig.18). The same samples are used for testing compression and flexing, but two compression values are obtained for each flexion value, one at 7 days and the other at 28 days

Each one of the halves of the test tubes is placed at the base of the device, with dimensions of 40x40 mm, and consisting of 3 pivots for the correct alignment of the sample. A load of 20kN has been applied at a speed of 240 kg·s-1 until the fracture of the sample. The calculation for the compression resistance is performed following the equation 6.

$$CS = \frac{\mathrm{F}}{\mathrm{b \cdot d}} \quad (6)$$

This testing follows the UNE-EN 196-1 regulation. The sample is positioned with the marked face perpendicular to the axis of compression.

Figure 18. Compression testing device

6. RESULTS AND DISCUSSION

The results of the tests described in the previous section are analyzed and discussed below.

6.1. FORMULATIONS

As was stated earlier, the priority of this study is to incorporate the maximum quantity of CSP while maintaining workability and setting time. To do so, 16 initial proposals were formulated as shows table 5.

Table 5. Initial formulations

Run	W/C	CSP (%)
1	0,38	0,00
2	0,38	0,00
3	0,34	4,86
4	0,34	0,47
5	0,36	8,57
6	0,38	15,00
7	0,34	15,00
8	0,36	15,00
9	0,38	7,50
10	0,35	9,38
11	0,35	0,00
12	0,38	15,00
13	0,34	0,47
14	0,37	0,70
15	0,34	15,00
16	0,38	7,50

There are some runs that are repeated because DoE also takes into account the repeatability of some formulations to know the human error and carry out the plot surface correctly. For the same reason ,the samples also need to be made in order.

6.2. PROPERTIES RESULTS

6.2.1. Contraction and apparent density

During the curing process the samples lose water and often they expand or shrink depending on the system that forms them. In this section the changing dimensions of the samples are followed. The base and the length of the sample is measured at 24 hours and at 7 days to determine the retraction that the material has.

Unfortunately, the results are inconclusive. A formulation expands while the same repeated formulation shrink. The results do not follow any coherent trend. The results of apparent density are shown in the table below.

Table 6. Apparent density results

Run	Density (g/cm^3)	Run	Density (g/cm^3)
1	1,797	**9**	1,806
2	1,783	**10**	1,880
3	1,826	**11**	1,819
4	1,800	**12**	1,859
5	1,830	**13**	1,802
6	1,826	**14**	1,826
7	1,881	**15**	1,890
8	1,835	**16**	1,871

The higher value is the one with less W/C ratio and more CSP percentage while the less dense is the one with less content of CSP.

The interaction model obtained from DoE presents no lack of fit with the data obtained from testing. The surface plot of density is shown in figure 19 and presents the following equation 7.

$$\text{Density}\left(\frac{\text{g}}{\text{cm}^3}\right) = 1{,}97 - 0{,}45\left(\frac{\text{W}}{\text{C}}\right) + 0{,}0037\text{CSP} \quad (7)$$

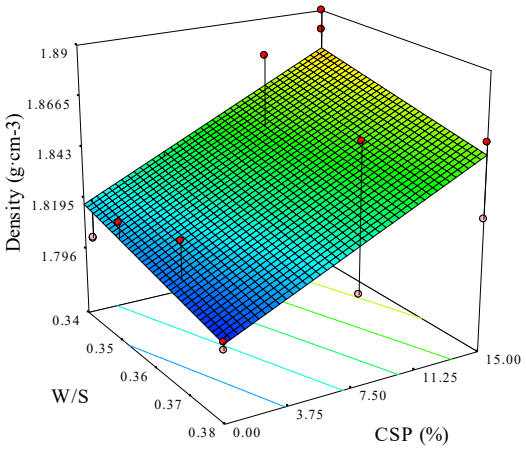

Figure 19. Surface plot of density as a function of W/C ratio and CSP.

CSP is significant and grows linearly. It is determined that W/C ratio is not significant. This can be justified because the range of W/C ratio is very short while the CSP range is wider.

These results are not taken into consideration when looking for the optimal formulation but the intervals obtained in it will be taken into account.

6.2.2 Modulus of Elasticity (MOE)

Below are the results of the average MOE values of each formulation obtained by ultrasound pass rate at the age of 7 days.

Table 7. MOE results

Run	MOE (GPa)	Run	MOE (GPa)
1	10,61	**9**	10,37
2	10,20	**10**	12,66
3	12,76	**11**	11,78
4	12,83	**12**	10,70
5	11,90	**13**	12,60
6	11,89	**14**	10,10
7	14,37	**15**	14,20
8	13,57	**16**	10,70

When the material is less porous and has a higher compaction, it is more dense, and the propagation of the waves are faster, so the material will be more rigid and the modulus of elasticity will be higher.

As it is shown in figure 20 and mathematically described in equation 8, CSP and W/C are significant but there is no interaction between both factors in the range under study for the MOE results.

$$\mathrm{MOE(GPa)} = 34{,}99 - 66{,}07\left(\frac{\mathrm{W}}{\mathrm{C}}\right) + 0{,}11\mathrm{CSP} \quad (8)$$

MOE increases as the quantity of CSP is higher since more heat is released, less water evaporates and the material is less porous and more rigid.

In addition MOE decreases as the W/C ratio increases, which might lead to porous formulations.

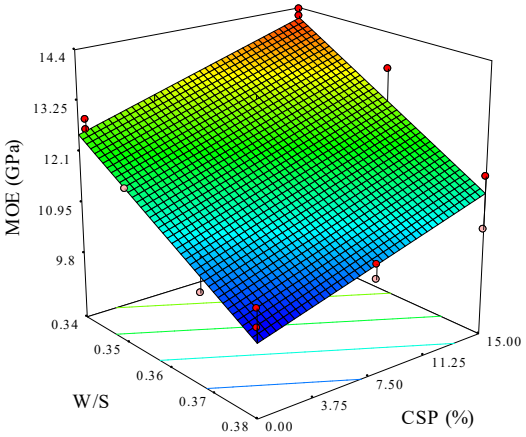

Figure 20. Surface plot of the modulus of elasticity as a function of W/C ratio and CSP.

6.2.3. Flexural Strength (FS)

The resistance to flexion of mortars is one of the most important mechanical property. Usually the measuring of flexural properties serve to analyze the capacity of the mortar to evacuate air. If air cannot be evacuated small vacancies in the form of pores can appear and can become cracks that can propagate if a tension is produced. This can also happen with water that does not react. The following results show the flexural strength of the samples obtained at 7 days.

Table 8. FS results

Run	FS (MPa)	Run	FS (MPa)
1	2,67	**9**	2,67
2	2,70	**10**	3,13
3	3,79	**11**	3,27
4	3,43	**12**	2,75
5	3,17	**13**	3,40
6	3,02	**14**	2,58
7	4,09	**15**	4,00
8	3,79	**16**	2,40

Significant statistical models are obtained for flexural strength and present no lack of fit. Both factors have a significant effect in the response but have no mutual interaction. The surface plot and the equation that follows are presented.

$$\text{FS (MPa)} = 12{,}15 - 25{,}55\left(\frac{\text{W}}{\text{C}}\right) + 0{,}03\text{CSP} \quad (9)$$

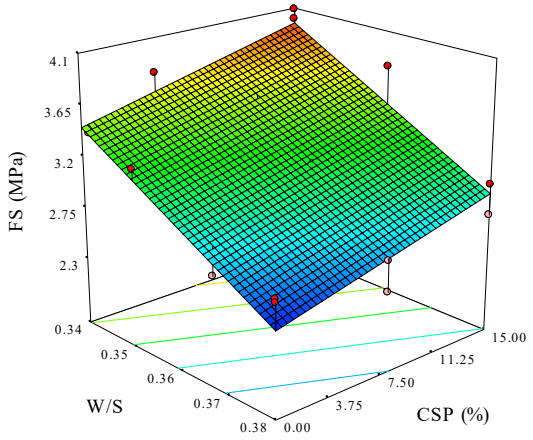

Figure 21. Surface plot of the flexural strength as a function of W/C ratio and CSP.

This surface plot reminds of MOE results. The linear dependence is the same, as the W/C ratio increases, the FS decreases.

This surface plot is only valid for the studied ranges, it cannot be said that to a greater quantity of CSP and less W/C ratio the material will have better properties to FS. We can only say for sure that up to 15% and 0,34 of W/C it does, these results cannot be extrapolated to a different ranges of the factors.

6.2.4. Compressive Strength (CS)

Resistance to compression is the most characteristic property of mortar and it is the one that is given most priority in order to determine the best formulation. Next are the results of the resistance to compression, obtained over a 7 day period.

Table 9. CS results at 7 days

Run	CS (MPa)	Run	CS (MPa)
1	11,58	**9**	10,30
2	11,30	**10**	15,00
3	14,07	**11**	13,80
4	15,75	**12**	10,80
5	12,75	**13**	15,20
6	11,89	**14**	9,76
7	18,03	**15**	18,00
8	14,20	**16**	11,08

In the case of testing a mortar to compressive stresses, the closing of the cavities is favoured and therefore the speed of propagation of the cracks decreases. This is why higher resistance values are obtained compared to flexural strength. Both surface plot and the equation that follows are shown below.

$$\text{CS (MPa)} = 512{,}47 - 2660{,}14\left(\frac{\text{W}}{\text{C}}\right) - 0{,}72\text{CSP} - 2{,}85\left(\frac{\text{W}}{\text{C}}\right)\cdot\text{CSP} + 3529{,}78\left(\frac{\text{W}}{\text{C}}\right)^2 + 0{,}33\text{CSP}^2 - 0{,}01\text{CSP}^3 \quad (10)$$

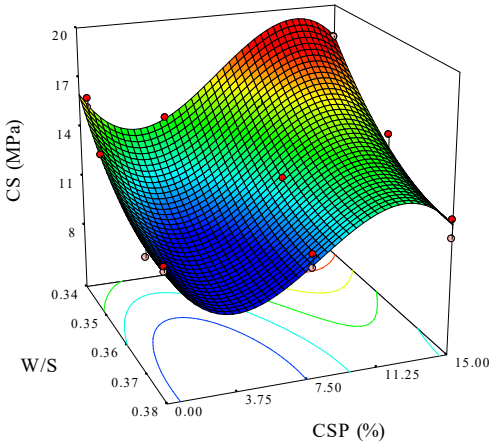

Figure 22. Surface plot of the compressive strength as a function of W/C ratio and CSP.

All parameters in the equation are significant unless (W/C)·CSP that the program cannot identify if it is significant or not. CSP has a higher importance than W/C ratio as it is elevated to the cube (Eq. 10).

The formulations that contain a higher water and CSP content have a lower compression value. The higher resistance to compression is found in formulations with 13% of CSP content and 0,34 W/C ratio.

Regulations use CS values at 28 days in order to determine what application can the material fit in. CS at 28 days are shown in table 10.

Table 10. CS results at 28 days

Run	CS (MPa)	Run	CS (MPa)
1	13,39	9	13,46
2	13,06	10	17,22
3	17,69	11	17,34
4	18,86	12	15,57
5	15,81	13	18,69
6	16,34	14	12,79
7	25,77	15	25,14
8	19,40	16	11,56

6.3. OPTIMAL FORMULATION

The analysis of DoE results is based on the analysis of variance (ANOVA). On the basis of the statistical analysis presented above, a numerical optimization is performed in order to obtain the optimal formulation for MPC. As mentioned before, the purpose of this analysis is to determine if there is synergy between both studied factors and obtain the formulation with the best properties. The basic concept of optimization entails a compromise between values.

Each property has been given a number of importance from 1 to 5, being 5 the most important. CS is treated as the most valuable property as it is the most characteristic in mortars and the one that is associated to its mechanical strength. The upper and lower limits are the values obtained from the tests (table 11).

The goal is to maximize the mechanical properties while keeping in range the two studied factors (CSP and W/C ratio). As it is mentioned in section 6.2.1. density values cannot be use to analyze due to a short range of W/C ratio compared with CSP percentage.

Table 11. Optimization criteria used in this study.

Constraints	Goal	Limits		Importance
		Lower	Upper	
W/C (%)	is in range	0,34	0,38	3
CSP	is in range	0	15	3
CS (MPa)	maximize	9,757	18,027	5
MOE (GPa)	maximize	10,101	14,365	1
FS (MPa)	maximize	2,4	4,09	1
Density (g/cm^3)	is in range	1,79652	1,89	3

Once we have the criteria, the program responds with the optimal formulations and its desirability (table 12).

Table 12 Optimal formulations

Number	W/C	CSP	CS	MOE	FS	Density	Desirability
1	0,34	15	18,08	14,1584	3,962	1,872	0,982
2	0,34	0	16,06	12,529	3,465	1,817	0,712

The optimal formulation with a 98.2% of desirability matches with the formulations 7 and 15, so it is not necessary to prepare them again because we already know their properties.

The formulation is optimal if it has 95% of the properties of the most desirable formulation, that is to say that all formulations that fall within the ranges of table 13 will be considered optimal.

Table 13. Optimal formulation ranges

Response	Prediction	95% CI low	95% CI high
CS	18,085	17,18	18,99
MOE	14,158	13,63	14,69
FS	3,9625	3,71	4,21
Density	1,872	1,85	1,9

The prediction values are the ones of the 7 and 15 formulation. Thus DoE validates this formulation since it is the only one that is in these ranges.

As the setting time is very short (a few minutes) the ideal application of the obtained material is as repairing mortar. The optimal formulation reaches the value of 25,77MPa to CS. According to regulation UNE-EN 1504-3 it has to accomplish the 25MPa to CS at 28 days to be considered a structural repairing mortar of R3 class. So according to the obtained results this is the proposed application.

At the end of its life cycle, the MPC will be part of the construction and demolition waste (RCD). According to the regulations, RCD have the alternative of being reused in other applications in the construction sector, such as filling materials or aggregates in new concrete.

6.4. MPC CHARACTERIZATION

The optimal formulation and the one with no CSP are characterized in order to determine if CSP does react with k-struvite to form a new crystalline structure

6.4.1. X-ray diffraction (XRD)

Both formulations have been superimposed to check if there is a new peak.

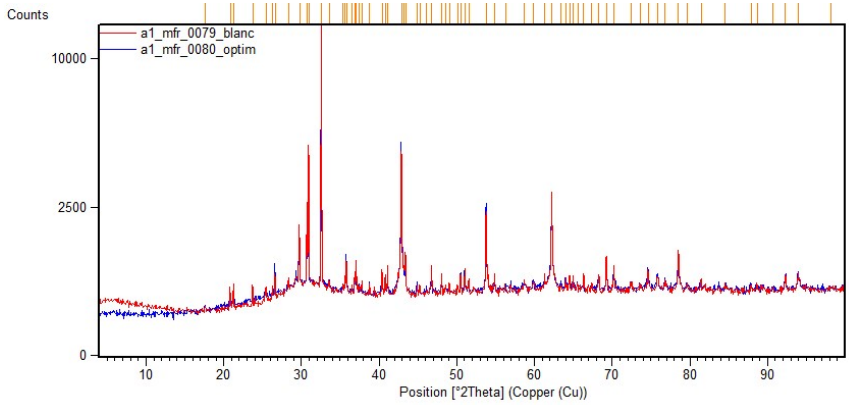

Figure 23 Diffractogram of both formulations

In figure 23 it can be distinguished that the main crystalline phases observed are k-struvite ($KMgPO_4 \cdot 6H_2O$), magnesite ($MgCO_3$), dolomite [$CaMg(CO_3)$], quartz (SiO_2),

periclase (MgO) and arcanite (K_2SO_4)). This last one is formed from the excess of MKP that has not reacted[18]. It should be noted that there are phases of the LG-MgO that have not reacted as well as the silica from the CSP.

6.4.2. Infrared Spectroscopy (FTIR-ATR)

IR is performed in the optimal formulation and the formulation with no CSP to observe new bands and therefore the certainty that new bonds are formed. The spectrum of both formulations is shown in figure 24.

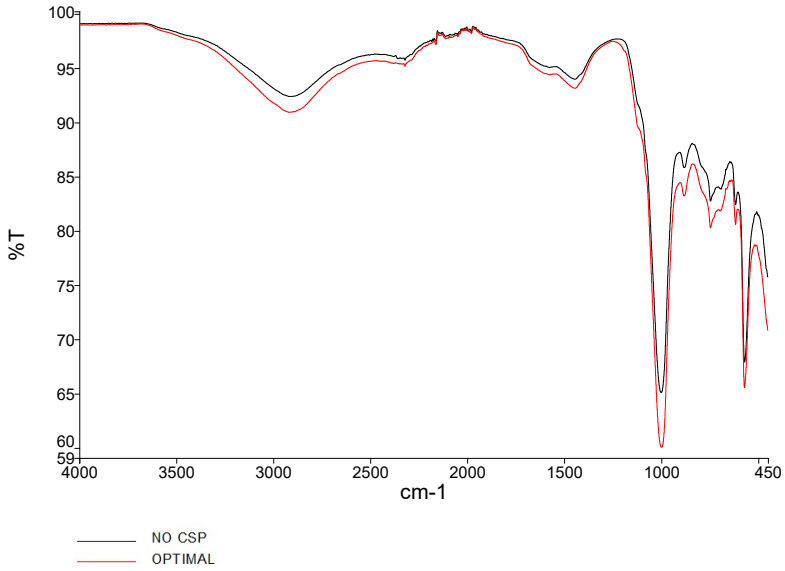

Figure 24. FTIR-ATR spectrum

Table 14 collects the information on each of the 5 bands that are identified in the spectrum and provide information on the composition of the material.

Table 14. Bonds and vibrational assignments of the samples

Observed wave numbers (cm-1)	Bonds/Vibrational assignments
3280 to 3550, 2358	H-O-H stretching vibrations of water
1600	H-O-H bending modes of vibrations
1016	Asymmetric stretching vibrations of PO_4
740	Oxygen-metal bond
571	Asymmetric bending vibrations of PO_4

IR spectroscopy confirmed the presence of k-struvite[19], by identifying stretching and bending vibrations of phosphate (PO_4) ions and Mg-O bond, as well as the presence of crystallization water molecules. The appearance or disappearance of significant enough bands is not appreciated to be able to claim that new bonds are formed or disappeared.

6.4.3. Scanning electron microscope (SEM)

SEM is used in order to observe the morphology of both formulations (optimal and the one with no CSP). Also energy-dispersive X-ray spectroscopy (EDS) is used to determine in a semi-quantitative way which of the elements are present. The detector of secondary electrons is used since the one of backscatered electrons, that gives us visual information of the heavy elements, is not relevant in this study. Figures 25a and 26b show the morphology and the present elements of the formulation with no CSP while figures 26a and 26b show the same for the optimal formulation.

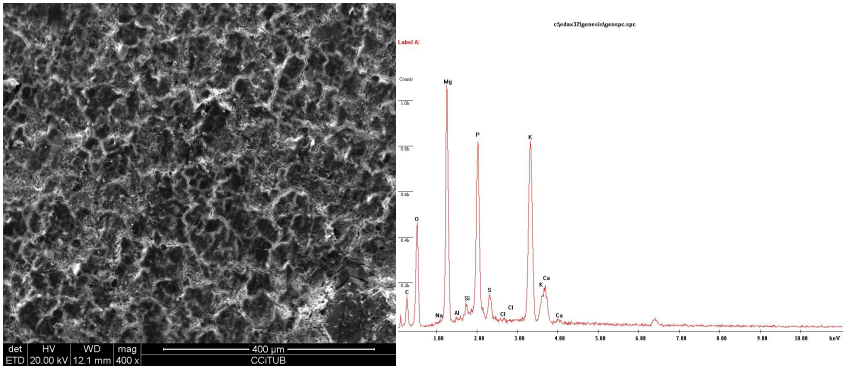

Figure 25 a) SEM image of the formulation with no CSP b) EDS spectrum

The sample is analyzed after the compression test, that is why microcracks can be observed that denote the stress to which the sample has been submitted.

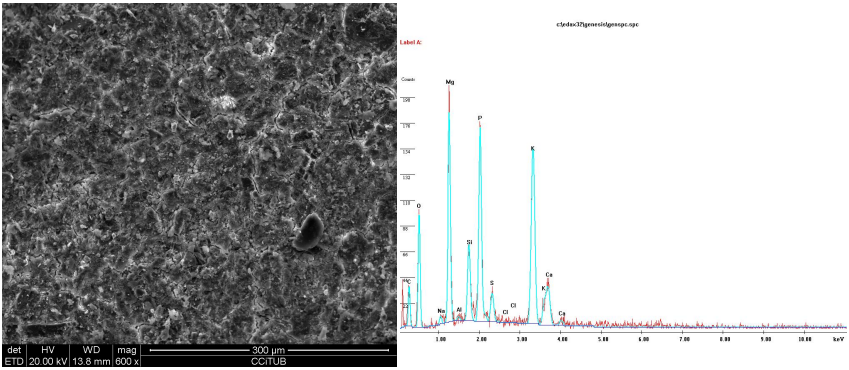

Figure 26 a) SEM image of the optimal formulation b) EDS spectrum

Both have parallel marks in the direction of sawing due to the preparation of the sample in order to be observed. The run with no CSP looks more cohesive than the optimal one. Besides, in the optimal formulation it can be seen a particle of CSP that is not part of the matrix. This inert particles reinforce the material and provide a higher strength to external stresses.

The only difference found in EDS is that the optimal formulation has a higher silicon peak. This is justified by the 15% of CSP content . The peaks of sodium and calcium should be higher .

7. ECONOMIC EVALUATION

In this chapter an economic valuation of the cost of the formulations of MPC is made as well as an estimate of the budget that this project has required.

7.1. ECONOMIC EVALUATION OF MPC

The cost of the raw materials used in this project is reflected in table 15. The approximate cost of a commercial MgO is also added to know the savings that it has meant working with Lg-MgO instead of pure MgO in obtaining the MPC.

It should be noted that the MPC obtained with pure MgO will not have the same properties as those obtained with LG-MgO, given that the pure MgO does not contain inert material that acts as a reinforcement in the chemical cement of phosphate.

Table 15. Raw materials cost

Raw Materials	Price (€/kg)
Lg-MgO (PC8)	0,19
KH_2PO_4 (MKP)	1,69
MgO	0,65
CSP	0,07
H_2O	0,000608

Pure MgO is 3.4 times more expensive than the magnesium by-product. The percentage of savings that the use of LG-MgO represents compared to pure MgO is 29.2%, a considerable saving that justifies the use of the magnesium by-product in obtaining the MPC. CSP is currently priceless but in the future it will have a cost. For this reason we consider the price of CSP to be the one that costs the transport, the trituration and milling (0,07 €/kg). It should also be taken into account that the cost of the formulation with pure MgO should be added the energy cost that would be the previous

calcination stage necessary to reduce the high reactivity that presents in the setting process. All the cost and quantities for MPC formulations made for this work are reflected in Table 16 to determine the total cost. The water cost is considered negligible and IVA is included.

Table 16. Material cost

	Run	kg	€/kg	€	Total(€)	Run	kg	€/kg	€	Total(€)
Lg-MgO	1	1,200	0,19	0,228	1,580	9	1,110	0,19	0,21	1,472
MKP		0,800	1,69	1,352			0,740	1,69	1,25	
CSP		0,000	0,07	0,000			0,150	0,07	0,01	
Lg-MgO	2	1,200	0,19	0,228	1,580	10	1,087	0,19	0,21	1,445
MKP		0,800	1,69	1,352			0,725	1,69	1,23	
CSP		0,000	0,07	0,000			0,188	0,07	0,01	
Lg-MgO	3	1,142	0,19	0,217	1,510	11	1,200	0,19	0,23	1,580
MKP		0,761	1,69	1,286			0,800	1,69	1,35	
CSP		0,097	0,07	0,007			0,000	0,07	0,00	
Lg-MgO	4	1,194	0,19	0,227	1,573	12	1,020	0,19	0,19	1,364
MKP		0,796	1,69	1,346			0,680	1,69	1,15	
CSP		0,009	0,07	0,001			0,300	0,07	0,02	
Lg-MgO	5	1,097	0,19	0,208	1,457	13	1,194	0,19	0,23	1,573
MKP		0,731	1,69	1,236			0,796	1,69	1,35	
CSP		0,171	0,07	0,012			0,009	0,07	0,00	
Lg-MgO	6	1,020	0,19	0,194	1,364	14	1,192	0,19	0,23	1,570
MKP		0,680	1,69	1,149			0,794	1,69	1,34	
CSP		0,300	0,07	0,021			0,014	0,07	0,00	
Lg-MgO	7	1,020	0,19	0,194	1,364	15	1,020	0,19	0,19	1,364
MKP		0,680	1,69	1,149			0,680	1,69	1,15	
CSP		0,300	0,07	0,021			0,300	0,07	0,02	
Lg-MgO	8	1,020	0,19	0,194	1,364	16	1,110	0,19	0,21	1,472
MKP		0,680	1,69	1,149			0,740	1,69	1,25	
CSP		0,300	0,07	0,021			0,150	0,07	0,01	
TOTAL COST 23,632€										

The total cost of all formulations is 23,632€. Also, the optimal formulation is the cheapest because it has the higher percentage of CSP.

7.2. BUDGET OF THE PROJECT

The following table shows an estimation of the budget that has involved the realization of this project in terms of the techniques used and the costs of human resources. It is considered that the student of the UB charges 8 € / h and the techniques used are subject to the tariff A, price of researchers.

Table 17. Total budget of the project

Activity	Nº tests	Time (h)	Unitary cost (€/h)	Total cost (€)
Trituration	1	4	10,2	40,8
Ball Mill		28	10,2	285,6
Ring Mill	53	5	6,99	34,98
Sifted		21	8,96	188,16
XRD	2	2	10,2	20,4
XRF	2	2	6,85	13,7
Granulometry	2	2	29,9	59,8
IR	2	2	21,72	43,44
SEM	2	2	19,06	38,12
MPC preparation		24	8	192
Determination of properties		28	8	224
Bibliographic search		12	8	96
Results analysis		60	8	480
Memory drafting		210	8	1680
TOTAL		**406**		**3397**

The total cost of this project is 3397€ and 406 hours have been invested performing it.

8. CONCLUSIONS

After carrying out all 16 formulations and performing different characterization techniques, the conclusions obtained in the work are exposed:

- A CSP and LG-MgO revaluation process has been achieved, which not only lowers the price of the final product but also promotes issues such as sustainability and the reduction of CO2 emissions due to the reduction in extraction pure MgO.
- There is a dependency between the W/C ratio and CSP content that is reflected in the data obtained from the mechanical properties and apparent density testing.
- DoE is performed successfully, presents no lack of fit with the data obtained from testing and gives us an optimal formulation with 0,34 W/C ratio and 15% of CSP content. This material can be applied as structural repairing mortar of R3 class.
- It is not clear that CSP reacts with k-struvite over time, it is possible that kinetic is slower. Therefore, it will be evaluated if it reacts in the long term, 1 month, 2 months, 3 months using the techniques of IR and XRD.

9. REFERENCES AND NOTES

1. Grau Torres P, Hernández Moreno M, Carreras Carrasco A. Reciclado y valorización de residuos en la industria cementera en España. *Cem hormigón*. 2009;930:44-86. http://www.fundacioncema.org/Uploads/docs/ES_Reciclado y valorizaci%F3n de residuos en la industria cementera %28periodo 2004-2006%29_F.CEMA.pdfhttp://www.fundacioncema.org/Uploads/docs/EstudioRV.pdf.

2. Ding Z, Li Z. High-early-strength magnesium phosphate cement with fly ash. *ACI Mater J*. 2005;102(6):375-381.

3. Abdelrazig BEI, Sharp JH, El-Jazairi B. The microstructure and mechanical properties of mortars made from magnesia-phosphate cement. *Cem Concr Res*. 1989;19(2):247-258. doi:10.1016/0008-8846(89)90089-6.

4. Yang Q, Zhu B, Wu X. Characteristics and durability test of magnesium phosphate cement-based material for rapid repair of concrete. *Mater Struct*. 2000;33(4):229-234. doi:10.1007/BF02479332.

5. García MM. Development of Magnesium Phosphate Cements as porous materials. 2017;(June). doi:10.1016/j.apcata.2017.03.016.

6. Maldonado Alameda A. Thermal and mechanical study of chemically bonded phosphate cements formulated with magnesium by-product incorporating phase changing materials. 2015. http://diposit.ub.edu/dspace/handle/2445/67213#.WrkCd1veqto.mendeley. Accessed March 26, 2018.

7. Wagh AS. *Chemically Bonded Phosphate Ceramics Twenty-First Century Materials with Diverse Applications*.; 2004. https://www.sciencedirect.com/science/book/9780080445052.

8. Antonio Bascones Martínez. *Tratado de Odontología Tomo LI Sección XVII Materiales Odontològicos*.; 2005.

9. Chauhan CK, Vyas PM, Joshi MJ. Growth and characterization of Struvite-K crystals. *Cryst Res Technol*. 2011;46(2):187-194. doi:10.1002/crat.201000587.

10. Graeser S, Postl W, Bojar H-P, et al. Struvite-(K), KMgPO4·6H2O, the potassium equivalent of struvite – a new mineral. *Eur J Mineral*. 2008;20(4):629-633. http://dx.doi.org/10.1127/0935-1221/2008/0020-1810.

11. Xu B, Ma H, Shao H, Li Z, Lothenbach B. Influence of fly ash on compressive

strength and micro-characteristics of magnesium potassium phosphate cement mortars. *Cem Concr Res*. 2017;99:86-94. doi:10.1016/J.CEMCONRES.2017.05.008.

12. Rodriguez Vietitez E, Eder P, Villanueva A, Saveyn H. *End-of-Waste Criteria for Glass Cullet: Technical Proposals*. https://www.researchgate.net/publication/265491948_End-of-Waste_Criteria_for_Glass_Cullet_Technical_Proposals.

13. Dias N, Garrinhas I, Maximo A, Belo N, Roque P, Carvalho MT. Recovery of glass from the inert fraction refused by MBT plants in a pilot plant. *Waste Manag*. 2015;46:201-211. doi:10.1016/J.WASMAN.2015.07.052.

14. Ruth M, Dell'Anno P. An industrial ecology of the US glass industry. *Resour Policy*. 1997;23(3):109-124. doi:10.1016/S0301-4207(97)00020-2.

15. Jacquez JA. Design of experiments. *J Franklin Inst*. 1998;335(2):259-279. doi:10.1016/S0016-0032(97)00004-5.

16. Lendrem D, Owen M, Godbert S. *DOE (Design of Experiments) in Development Chemistry: Potential Obstacles*. Vol 5.; 2001. doi:10.1021/op000025i.

17. Formosa J, Aranda MA, Chimenos JM, Rosell JR, Fernández AI, Ginés O. Cementos químicos formulados con subproductos de óxido de magnesio. *Bol la Soc Esp Ceram y Vidr*. 2008;47(5):293-297.

18. Formosa Mitjans J. Formulaciones de nuevos morteros y cementos especiales basadas en suproductos de magnesio. December 2012. http://diposit.ub.edu/dspace/handle/2445/36456#.WrkC0ZnQE2E.mendeley. Accessed March 26, 2018.

19. Suryawanshi VB, Chaudhari RT. Synthesis and Characterization of Struvite-k Crystals by Agar Gel. *J Cryst Process Technol*. 2014;4(4):212-224. doi:10.4236/jcpt.2014.44026.